International Journal of GEOMATE, March, 2018 Vol.14, Issue 43, pp.1-7
Geotec., Const. Mat. & Env., DOI: https://doi.org/10.21660/2018.43.3530
ISSN: 2186-2982 (Print), 2186-2990 (Online), Japan

FINITE ELEMENT ANALYSIS OF EWECS COLUMNS WITH VARYING SHEAR SPAN RATIO

*Fauzan[1], Ruddy Kurniawan[2], and Zev Al Jauhari[3]

[1,2,3] Engineering Faculty, University of Andalas, Indonesia

*Corresponding Author, Received: 1 July 2017, Revised: 25 Sept. 2017, Accepted: 1 Dec. 2017

ABSTRACT: A new hybrid structural column system called Engineering Wood Encased Concrete-Steel (EWECS) column was developed for low and high seismic zones. Experimental studies on the seismic behavior of EWECS columns with varying shear span to depth ratio (shear-span ratio) have been conducted by one of the authors. To complement and validate the experimental program, finite element analysis (FEA) on EWECS columns with varying shear-span ratio ranging 1.0 to 2.0 under constant axial and lateral cyclic loads are summarized. This numerical analysis uses finite element program, ANSYS APDL v.14, to investigate the structural performance of the EWECS columns, which was compared with the experimental results. A detailed three-dimensional (3D) nonlinear FE model of three EWECS columns with varying shear-span ratio, subjected constant axial and lateral cyclic loads are performed. The FEA results showed that the shear-span ratio affected by the maximum shear strength and failure mode of the EWECS columns. The maximum strength of the columns increased with decreasing shear-span ratio. The stress distribution on the FE models represented the failure mode of the EWECS columns well. More damages on the columns were observed with decreasing shear-span ratio. In general, good agreement between the experimental data and the FE models output in terms of the seismic performance and failure mode was observed.

Keywords: Column, Composite structure, Finite element analysis, ANSYS, Seismic performance.

1. INTRODUCTION

It has been known that the composite steel-concrete columns such as Steel Reinforced Concrete (SRC) and Concrete Filled Tube (CFT) columns have been widely used in high-rise and long-span buildings. Based on the ideologies of SRC and CFT composite columns, a new hybrid structural column system called Engineering Wood Encased Concrete-Steel (EWECS) column was developed for low and high seismic zones. This new composite material overcomes the limitation of the stories number that can be constructed by utilizing wood as material on it. This column consists of concrete encased steel (CES) core wrapped with an exterior wood panel [1], as shown in Figure 1.

The wood panel as column cover in EWECS column has some benefits. It does not only improve the structural behavior through its action to provide core confinement and resistance to bending moment, shear force, and column buckling but also reduce the cost and time of construction.

An experimental study on EWECS columns with varying shear-span to depth ratio ranging from 1.0 to 2.0 under constant axial and lateral load reversals was conducted to obtain the effects of shear span to depth ratio on the seismic behavior of EWECS columns [1].

To complement and validate the experimental program, a 3D finite element (FE) model of EWECS columns with varying shear span to depth ratio using ANSYS APDL 14.0 software [2] was developed. The developed model takes into consideration the nonlinear behavior of material [3]. The results of the numerical simulation are compared with the experimental test results. In this paper, the shear span to depth ratio will subsequently be referred to as "shear-span ratio".

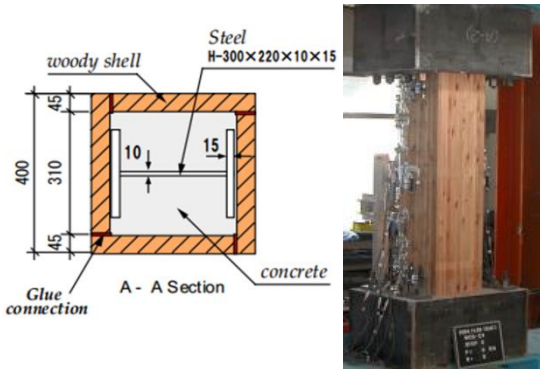

Fig. 1 Specimen detail of EWECS column [1]

2. THE GEOMETRY AND ELEMENT TYPE OF 3D FE MODEL

A three-dimensional finite element model of the tested system has been developed via the Finite Element Package ANSYS APDL v.14 [2] to detect

in detail the local and global behavior of EWECS columns. A total of three EWECS column models with varying shear-span ratios are performed. The cross-section of all the columns is 1600 mm^2 and different shear-span ratios (1.0, 1.5 and 2.0) are achieved by varying the height of the columns (800 mm, 1200 mm and 1600 mm), as shown in Table 1. The details and names of the 3D FE models in terms of the geometry of steel section, concrete, and wood panel are generated and described in Figure 2.

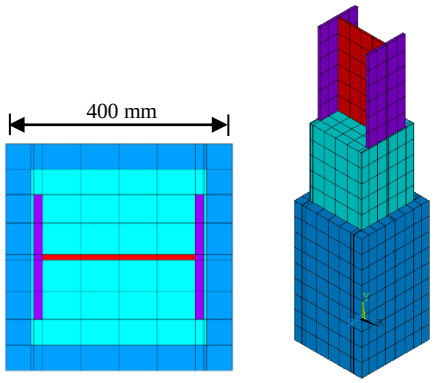

Fig. 2 The 3D FE model of EWECS column

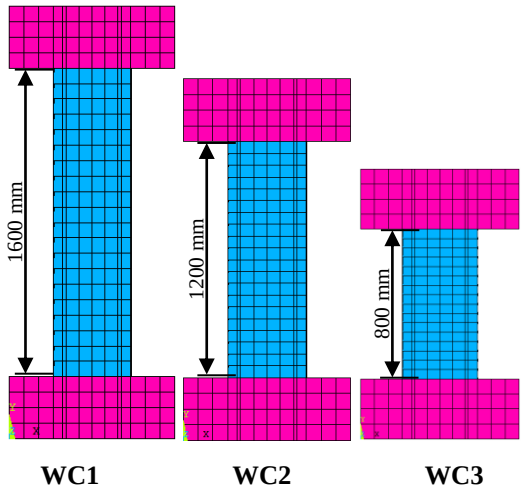

Fig. 3 Full models of EWECS column with varying shear-span ratio

Table 1 FE models

Shear-span ratio	Model	Height (mm)
2	WC1	1600
1.5	WC2	1200
1	WC3	800

The steel encased in each column has a single H-section steel 300 x 220 x 10 x 15 mm. The specimen is covered by a wood panel with a 45 mm thickness, while the core section is concrete encased steel. The FE models are developed to accurately represent the geometrical configuration and dimensions of the test specimens. The EWECS columns with varying shear-span ratio are modeled as a block and solid cube with an equivalent length to represent the total area of the specimen, as illustrated in Figure 3.

The discretization of the tested EWECS columns is made of SOLID elements; each element has eight nodes with three degrees of freedom on each node. ANSYS solid element, SOLID185 is used to modeling the steel section and wood panel, while SOLID65 is used for modeling the concrete of the EWECS columns.

The FE model in this study is considered perfectly-bonded for the material interface between steel and concrete, while unbonded for the material interface between wood and concrete is performed by slightly reducing the constitutive model of wood panel. This assumption is applied because bonded and unbonded between adjacent materials (wood and concrete) do not much influence for flexural capacities of the columns in the previous experimental study [4].

3. MATERIAL PROPERTIES, MESHING, LOAD, AND BOUNDARY CONDITIONS

3.1 Material Properties

3.1.1 Concrete

Nominal compressive strength 35 MPa with a peak concrete strain 0.0025 was used for all models. Figure 4 shows the tensile stress-strain curve for the concrete. The stress-strain relationship is designed on the concrete model that developed by Saenz [5]. The tensile relaxation (softening) is presented by a sudden reduction of the tensile strength to 0.6 x f_r upon reaching the tensile cracking strain, ε_{cr}. After this point, the tensile response decreases linearly to zero stress at a strain of 6 x ε_{cr}, as shown in Figure 5.

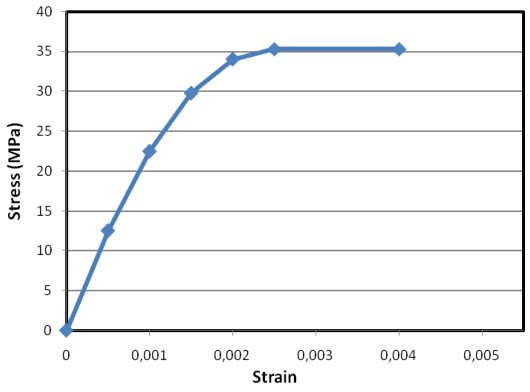

Fig. 4 Compressive stress-strain curve for concrete

A shear transfer model developed by Al-Mahaidi [6] is added in the analysis, with value

0.75 and 0.9 for β_t and β_c, respectively. The fracture criterion of concrete is adopted the five parameter model of William-Warnke [7].

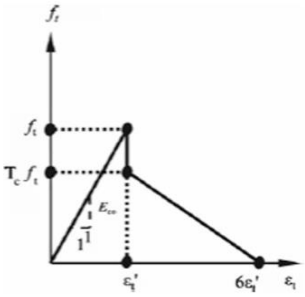

Fig. 5 Tensile stress-strain curve for concrete [5]

3.1.2 Encased steel

The yield strength of the steel used in each model is 293.6 and 313.3 MPa for flange and web steel, respectively. In this study, the constitutive model of the steel used is a perfectly elastic-plastic criterion. At first, this curve is elastic, then it is assumed perfectly plastic (bilinear isotropic model), as shown in Figure 6.

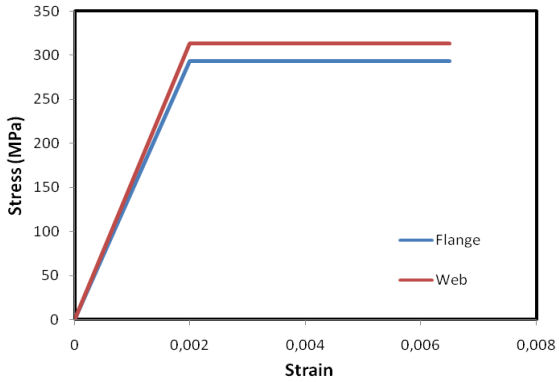

Fig. 6 Tensile stress-strain curve for steel

3.1.3 Wood panel

The compressive strength and modulus elasticity of wood panel are 46.2 MPa and 13700 MPa, respectively. The constitutive model of engineering wood panel is shown in Figure 7. The stress-strain relationship in the rising region was modeled with the linearly increasing model by slightly reducing (5%). The fracture criterion of wood is adopted by following the rule of William-Warnke's five parameter model [7] for concrete by being input wood material characteristic. The maximum tensile strength of the wood panel during the analysis was taken 5 MPa. This value is taken into consideration the lower tensile strength in the direction perpendicular to the grain. The shear transfer model for concrete developed by Al-mahaidi [6] was included by using modified shear transfer coefficient, β_c, of 0.35 for wood.

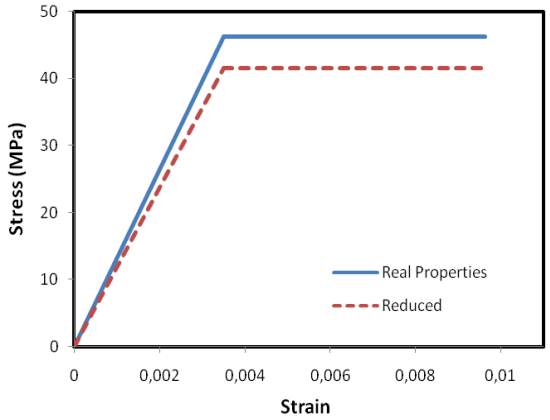

Fig. 7 Tensile stress-strain curve for wood

3.2 Meshing

The mesh density was chosen so that the elements aspect ratio is nearly equal to one. This provided adequate accuracy and fair computational time in modeling the EWECS columns. The total numbers of element used are 5095, 4820, 4570 for WC1, WC2, and WC3, respectively. This is an adequate refinement for constructing the 3D FE models.

3.3 Boundary Conditions

The boundary conditions in FE models were corresponding to the experimental setup (Figure 8). An anchor plate/ stub (700.700.400 mm) was used in the model at the top and bottom of the column. Nodes at the bottom of the column are restrained in all DOF, and the top of the column is restrained in the vertical y-direction. The vertical y-direction is restrained because the column prevents any displacement in this direction. The nodes at the two edge lines of the column are coupled in the lateral x-direction to ensure all nodes associated with this line that move together. The final boundary conditions of FE model is shown in Figure 9.

Fig. 8 The setup of experimental study [1]

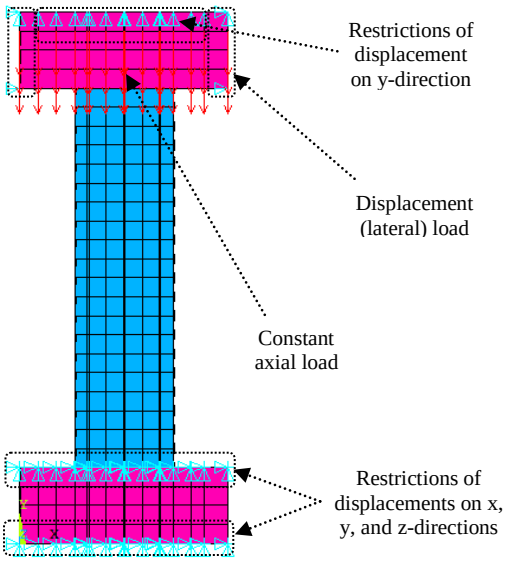

Fig. 9 Boundary conditions of FE model

3.4 Loads

The loading in the study was applied as follows: constant axial load, approximately 1031 kN, was applied to the top face of the column. This is represented in the FE model by applying a point pressure 1.4 kN on the upper elements (steel plate) of a total nodal area 717. The loading history for the model is based on story drift and is the one recommended for use in the experimental study [1]. This is represented in the FE model by applying the displacement in cycles of loading and unloading at the top edge of the column. The incremental loading cycles were controlled by story drift, R, defined as the ratio of lateral displacements to the column height, δ/h. The lateral load sequence consisted of one cycle to each story drift, R of 0.5, 1, 1.5, 2, 3 and 4% followed by half cycle to R of 5%, as shown in Figure 10. It should be noted that the cyclic lateral loads were different for each model.

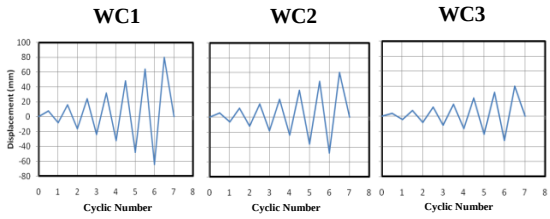

Fig. 10 Lateral cyclic load history

Before the analysis of the program, the appropriate loading steps and the number of iteration were set. The applied cyclic displacements are divided into a series of increments called load steps and load sub-steps [8]. The automatic time stepping option is enabled in this analysis to predict and control the load step size increments. In this study, the convergence criteria for the elements are based on displacement. ANSYS convergence tolerance default values 5% for displacement checking are initially selected. It is found that convergence is difficult to achieve using the default values due to the associated large deflections and the highly nonlinear behavior of the concrete elements. Thus, in order to obtain convergence of the equilibrium iterations, the convergence tolerance limits are increased to 15% for the displacement checking criterion [9].

4. RESULT AND DISCUSSIONS

4.1 Hysteresis Characteristics

The comparison of shear versus story drift relationships between all specimens and FE models are plotted in Figure 11. The blue dotted and red lines are drawn in this figure represent the hysteresis loops of the specimens and FE models of EWECS columns, respectively.

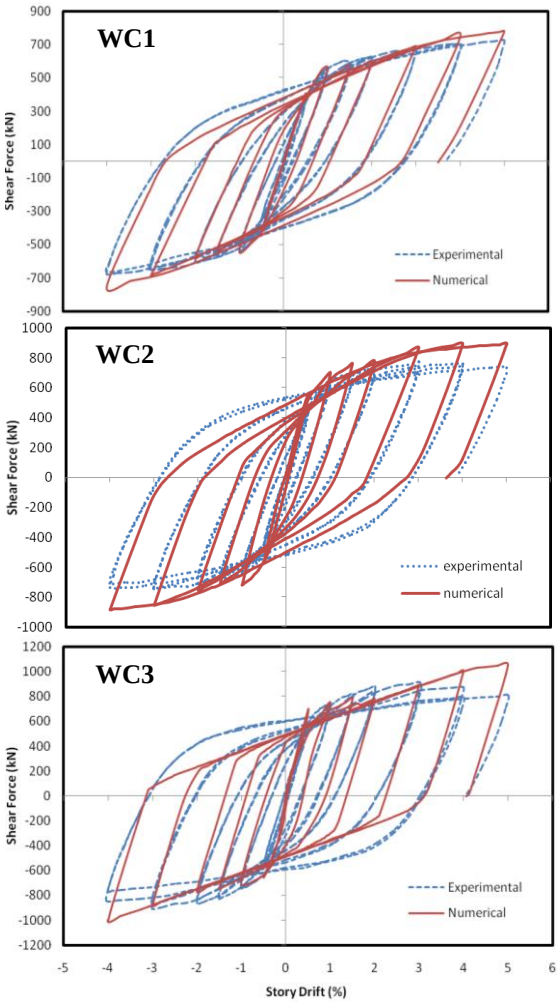

Fig. 11 Comparison of hysteresis loops between experimental and numerical results

The yield and maximum strengths and the corresponding story drift for each specimen are listed in Table 2. The yielding of each specimen was assumed when the first yielding of steel flange or web at the top and bottom of columns was observed, while the yielding of FE model was observed when the principal strain in the encased steel was reached about 0.002, as seen in Figure 12.

From Figure 11, it can be seen that all the specimens and FE models showed ductile and stable spindle-shaped hysteresis loops for WC1 and WC2, while for WC3 showed a slight pinching-shaped. In Model WC1 with a shear-span ratio 2.0, the first yielding occurred on steel flange when the applied load was 367 kN and R 0.55%, while in the test specimen, the first yielding occurred on steel flange at R 0.5%. The maximum capacity of the FE model was reached in the last story drift of 778 kN, while the maximum capacity was 725 kN in the test specimen. This was approximately 6.8% higher than the results obtained from the experiment.

For Model WC2 with a shear-span ratio 1.5, the first yielding also occurred on steel flange at a shear force 454 kN and R 0.49%, while in the specimen, the first yielding occurred on steel flange at R 0.5%. The maximum capacity of 926 kN was reached at R 5%, which was approximately 13% higher than the results obtained from the experiment. Good correlation exists in initial stages (R 0.5% - 3%) of lateral cycling loads.

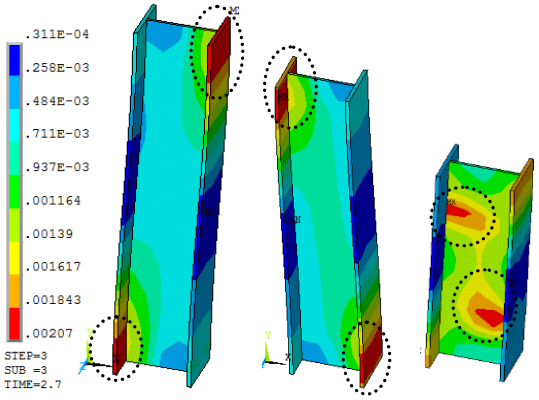

(a) WC1 (b) WC2 (c) WC3

Fig. 12 The principal strain at first yielding of the FE models

Model WC3 with the smallest shear-span ratio showed the highest maximum capacity among the simulated models. However, the yielding location of the FE model was different from the other two models. The first yielding of the model occurred on the steel web at a shear force 613 kN and R 0.58%, while in the FE model, the first yielding occurred on steel web at R 0.64%. The maximum capacity was reached at shear force 1022 kN and R 5% in the FE model, which was approximately 10.3% higher than the maximum capacity of the test specimen.

Table 2 Comparison of measured strength between experimental specimens and FE models

Model	Study	At Yielding		Max. Capacity	
		Qy (kN)	Ry (%)	Qmax (kN)	Rmax (%)
WC1	Exp.	386	0.5	725	5
	Num.	367	0.55	778	5
WC2	Exp.	423.1	0.5	797	3
	Num.	454	0.49	926	5
WC3	Exp.	666.2	0.64	916	3
	Num.	613	0.58	1022	5

4.2 Failure Mode

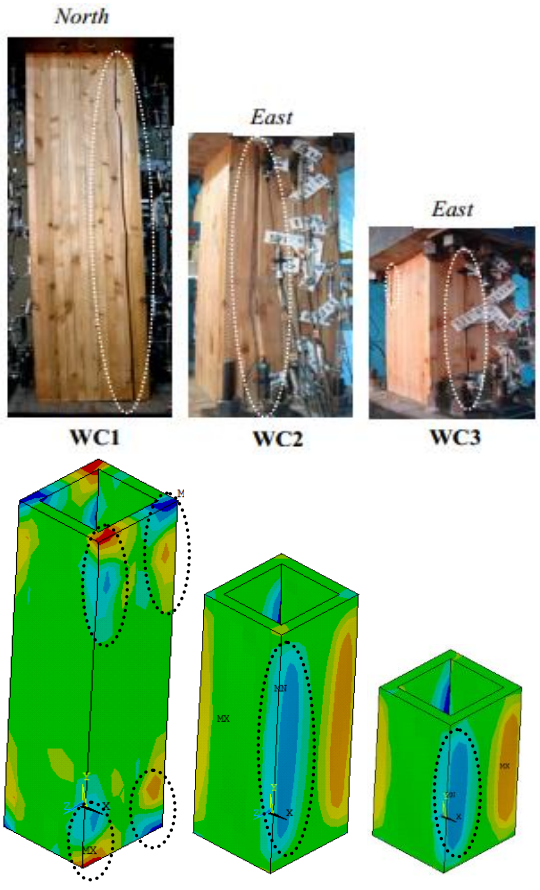

Fig. 13 Comparison of failure mode of wood panel between experimental and FEA results

Figure 13 shows the comparison of the failure mode of the wood panel between experimental and FEA results. In Model WC1, the first cracks in the wood panel occurred in the North and South side

of the column face at around 35 cm away from the top of the column. The cracks are indicated by the principal shear stress in the wood that was higher than the tangential shear strength of the wood suggested by Calderoni [10]. It was average 7.44 MPa at the location where the wood panel of the column was assembled together by using wood glue, as seen in Figure 13. This is also seen on the test specimen, that the crack of wood panel occurred on the North side of the column face at around 30 cm away from the top of the column. The cracks are also formed on the opposite side of the column, and it propagated along the column height.

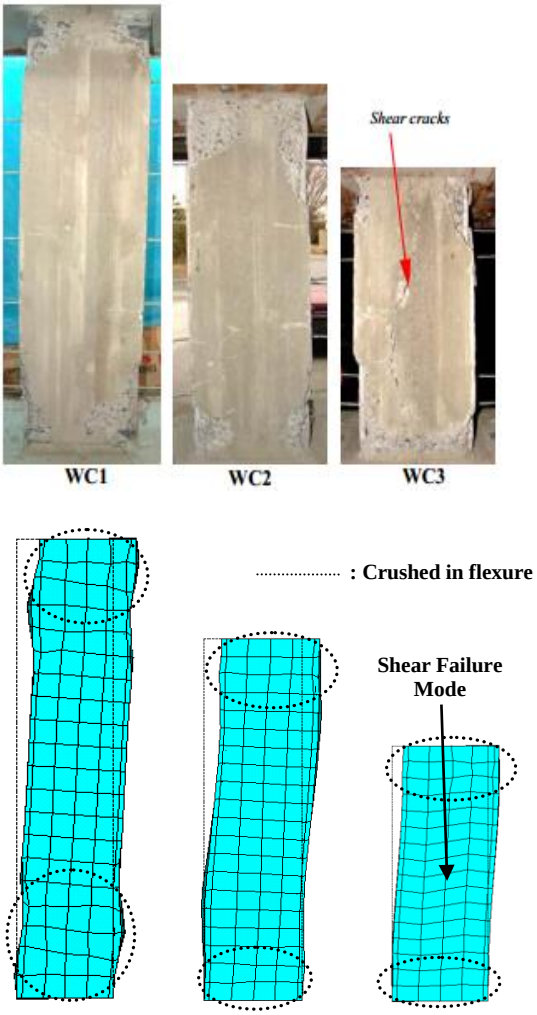

Fig. 14 Comparison of failure mode of concrete between experimental and FEA results

For Model WC2, the first cracks of wood panel occurred at R 3% on the East side of the column. In FE model, the cracks occurred on the wood panel at shear stress approximately 7.8 MPa.

In Model WC3, the first cracks of wood panel occurred at R 3% in the North side of the column as indicated by the principal shear stress in the wood approximately 7.3 MPa, while in the test specimen, first cracks occurred at R 2%. Subsequently, the cracks extended along the column height with the increase of story drift.

After testing, the wood panel was removed from the columns to inspect the damage of concrete visually. Figure 14 shows the comparison of the failure mode of concrete between experimental and FEA results. From the figure, it was observed for all models that the in-filled concrete had crushed in flexure at both the top and bottom of columns, which matched well with the tested specimens. In addition, shear cracks occurred along the column height in Model WC3 and no shear cracks were observed for the other two models.

5. CONCLUSION

(1) The hysteresis characteristics of the FEA correlated fairly well with the experimental results. The different percentage of the maximum flexural capacity between FE models and test data were 6.8%, 13%, and 10.3% for Model WC1, WC2, and WC3, respectively.
(2) FEA results indicated that the smaller shear-span ratio causes a higher shear force for the EWECS columns. The ultimate flexural strength of EWECS columns increased by reducing the shear-span ratio.
(3) The stress distribution on the FE models represented the failure mode of the EWECS column specimens well. The damage of the columns in the CES core became dominant as decreasing the shear-span ratio.

6. REFERENCES

[1] Fauzan, Kuramoto H., Matsui T., and Kim K. H., Seismic Behavior of Composite EWECS Columns with Varying Shear-Span Ratios, Proceedings of JCI, 28(2), 2006, pp. 1357-1362.
[2] ANSYS Version 14.0, User and Theory Reference Manual, 2004.
[3] Tanaka H. and Toi Y., Ultimate Strength and Fatigue Life of Concrete Elements Reinforced with Carbon Fiber Sheet Based on Continuum Damage Mechanics, Int. J. of GEOMATE, Vol. 2, No. 1 (Sl. No. 3), March 2012, pp. 171-178.
[4] Meas K., Fauzan, Matsui T., and Kuramoto H., Seismic Behavior of Engineering Wood Encased Concrete-Steel Composite Structural Systems, Part I: Effect of Shear Studs on Behavior of EWECS Columns, Proc., Architectural Institute of Japan, AIC, Tokyo, 2006, pp. 1181-1182.

[5] Saenz L. P., Discussion of Equation for the Stress-Strain Curve of Concrete, J. of American Concrete Institute, 61(9), 1964, pp. 1229-1235.
[6] Al-Mahaidi R. S. H., Nonlinear Finite Element Analysis of Reinforced Concrete Deep Members, Rep. No. 79-1, Dept. of Structural Engineering, Cornell Univ., Ithaca, NY, 1979.
[7] William K. L. and Warnke E. P., Constitutive Model for the Triaxial Behavior of Concrete, Int. Association for Bridge and Structural Engineering, Proc. Vol. 19, IABSE, Zurich, Switzerland, 1975.
[8] Zhang K., Yang Q., and Jiang J. C., Numerical Simulation of 2D Crack Growth with Frictional Contact in Brittle Materials, Int. J. of GEOMATE, Vol. 3, No. 1 (Sl. No. 5), Sept. 2012, pp. 339-342.
[9] Hawileh R. A., Rahman A., and Tabatabai H., Nonlinear Finite Element Analysis and Modeling of a Precast Hybrid Beam-Column Connection Subjected to Cyclic Loads, J. of Applied Mathematical Modeling, ScienceDirect 34, 2010, pp. 2562-2583.
[10] Calderoni C., Matteis G. D., Giubileo C., and Mazolani F. M., Flexural and Shear Behavior of Ancient Wood Beams: Experimental and Theoretical Evaluation, J. of Structural Eng., 28(5), 2006, pp. 729-744.